NASA Technical Memorandum 86360



# Impact Studies of a 1/3-Scale Model of an Air Cushion Vehicle

Robert H. Daugherty



APRIL 1985

NASA

NASA Technical Memorandum 86360

# Impact Studies of a 1/3-Scale Model of an Air Cushion Vehicle

Robert H. Daugherty
*Langley Research Center*
*Hampton, Virginia*

NASA
National Aeronautics
and Space Administration

**Scientific and Technical Information Branch**

**1985**

## Summary

An experimental investigation was conducted at the NASA Langley Research Center to determine the effects of various parameters on the impact performance of a 1/3-scale dynamic model of an air cushion vehicle. Impact response was determined by measuring the maximum values of variables, including side-lobe, front-lobe, and cavity pressures, normal acceleration, pitch and roll angles, and vertical displacement during impact, for various combinations of drop height, initial pitch and roll angles, and forward speed. Increasing initial pitch angle increased the maximum values of the front-lobe pressure, normal acceleration, nose-down pitch angle, and to some extent, vertical displacement, but it inversely affected the maximum cavity pressure. Increasing the drop height of the model increased the potential energy of the system and generally produced larger responses over the entire range of variables measured, except for the roll angle after impact, which remained constant. Forward speed had no effect on the impact performance of the model, except for essentially doubling the maximum nose-down pitch angle after impact at the maximum speed tested.

## Introduction

As potential applications for air cushion vehicles grow, the need to define their dynamic characteristics becomes greater. Increasing demands are imposed on these vehicles as their operating advantages are discovered and exploited. Potential uses of air cushions include public transportation, military platforms to transport conventional aircraft across bomb-damaged surfaces (ref. 1), landing systems for conventional or future aircraft (ref. 2), and icebreakers used to clear paths in previously unnavigable waters, especially in the Canadian environment (ref. 3). In each of these uses, vertical impacts are experienced to some degree. A knowledge of the peak magnitudes of the pressures and accelerations of an air cushion vehicle undergoing various impacts would be useful. Designers of future air cushions need to know the magnitudes of these parameters in order to design a system capable of accommodating the loads and impacts anticipated during normal and emergency operations.

The purpose of this paper is to present results of an experimental program conducted at the NASA Langley Research Center in which a scale model of an air cushion vehicle was subjected to vertical impacts for a variety of initial conditions. This vehicle was equipped with a unique, four-lobed air cushion designed as an aircraft landing system. A 1/3-scale dynamic model of the modified airboat described in reference 4 was fabricated and tested at forward speeds from 0 to 15 ft/sec. The model was dropped vertically from heights up to 6 in. to give an impact speed of up to 5.7 ft/sec, which represents an impact speed of up to 9.8 ft/sec for a full-scale vehicle. Although the impact speed is representative of full-scale conditions, the forward speed is not. Aircraft wing lift was not simulated for these tests. The model was dropped with initial pitch and roll attitudes ranging from 0° to 15° and 0° to 5°, respectively. The parameters measured during this investigation included side-lobe, front-lobe, and cavity pressures, normal acceleration, pitch and roll angles, and vertical displacement.

## Apparatus and Test Procedure

### Test Facility

All tests in this investigation were conducted at the Langley Aircraft Landing Dynamics Facility. This facility is composed of a propulsion system, a track, an arrestment system, and a carriage. The 2200-ft long track consists of two rails 30-ft apart, with a runway between the rails. A detailed description of this facility can be found in reference 5. The model tests were conducted in a towing basin adjacent to the main track. Figure 1 is a photograph of the model on its support sting. The water basin, which was empty for this test, is 8 ft wide, 6 ft deep, and extends the length of the track. A 4-ft wide, 200-ft long wooden runway was fabricated in the bottom of the basin to provide a smooth, level surface on which to land the model. The model was supported by the carriage, using a cantilevered structure which overhung the basin and to which the model support sting was attached. In tests when forward speed was needed, the carriage was towed by a tug.

### Model

The model used in this investigation was a 1/3-scale dynamic model of a full-scale modified airboat used in previous air cushion studies (ref. 4). A photograph and a sketch of the model are shown in figure 2. The model base consisted of a 3-ft by 5-ft aluminun honeycomb sandwich that was 2 in. thick. A four-lobed air bag was attached to the base, and holes were cut in the base to allow air from the feed hoses to flow to the lobes. The air bag consisted of polyurethane-coated Kevlar, and was similar in construction to the one described in reference 4, except that a thinner material was used. The rectangle described by the four lobes of the model air bag measured 33 in. by 59 in. The volume surrounded by the four lobes is referred to as the

cavity. Each lobe had peripheral holes at the ground tangent to allow air to escape and lubricate the air-bearing surface. A tip-turbine fan was mounted on the rear of the model to provide airflow to the air bag. High-pressure nitrogen stored on the carriage was metered to the tip-turbine fan, causing it to rotate and draw in ambient air. This air was then distributed from a plenum to each of the four air-bag lobes.

A heave pole (2 in. by 4 in. by 5 ft) was mounted on gimbals at the center of gravity of the model shown in figure 3. The heave pole was guided vertically by bearings mounted in a roller cage, allowing free vertical motion while restraining the model in fore-and-aft and lateral motion. The gimbals allowed the model to pitch and roll freely about its center of gravity at the base of the heave pole.

Also shown in figure 3 are roll and pitch bars, used to restrain roll and pitch motion until just before model impact. Bars of various lengths were pinned in a clevis arrangement on the heave pole. Cables attached to the pins were sized in length so that as the model neared the ground during a test, the cables would pull the clevis pins, which would allow springs to pull the roll and pitch bars clear of the heave pole and permit roll and pitch motion. Pitch bars were sized to provide initial pitch attitudes of 0°, 5°, 10°, and 15° nose-up. Roll bars were sized to provide initial roll attitudes of 0° and 5°.

Lead weights (fig. 3) were sized and placed to complete the dynamic scaling of the model. The weights were necessary to accurately model full-scale vehicle mass and pitch and roll inertias. Table I presents the scaling laws used. These laws are identical to those used in the investigation described in reference 6. Table II presents full-scale vehicle and model information.

### Instrumentation

Parameters measured during each test included side-lobe pressure, front-lobe pressure, cavity pressure, tip-turbine fan dynamic pressure, normal acceleration, pitch and roll attitude, vertical displacement, and forward speed. Pressures and accelerations were measured using conventional strain-type transducers. Pitch and roll attitudes were measured using rotational potentiometers mounted on the appropriate pivot axis at the center-of-gravity gimbals. Vertical displacement was measured using a slide wire. Forward speed was measured using a dc generator driven by one of the carriage wheels.

All measurements of these parameters were recorded on a 14-channel analog FM tape recorder. After a test run, the recording was played back into an oscillograph, and the data were recorded on paper for later analysis.

### Test Procedure

For each test, the model was raised to the desired drop height with a winch. An electrically operated bomb release was attached to the end of the winch cable and held the heave pole, which supported the model. Figure 4 shows the bomb release and the heave pole. In all tests, drop height is defined as the height above the runway to the nearest portion of the air bag; hence, when the model was initially at a pitch angle, the center of gravity was higher than it would be at the same drop height with 0° pitch angle. The pitch and roll bars corresponding to the desired initial conditions were installed, and the length of the cables to pull the clevis pins was set. Nose-up pitch and left roll are considered positive. At this point, the tape recorder was turned on. High-pressure nitrogen was metered through a regulator into the tip-turbine fan to spin it up and inflate the air bag. When the air flow was stabilized (approximately 2 seconds), the bomb release was activated to drop the model. After model motion stopped, the test was over.

The test procedure was identical for forward-speed tests, except that the nitrogen was introduced for a longer period of time to insure full inflation before the runway was encountered. When model pitch and roll motions ceased, the carriage was stopped quickly to minimize wear on the air bag.

## Results and Discussion

Data obtained from analysis of the tape-recorded tests are presented in table III. The table presents the initial conditions of each run, followed by maximum values of each of the measured parameters. Fan dynamic pressure was recorded during each test run, but is not presented in the table, since it was held constant for all tests at a dynamic pressure which produced a flow of 0.4 lbm/sec. The forward speed for each run is also presented; however, in approximately half of the forward speed tests, these data were not obtainable from the recording. Therefore, when the forward speed is not known, it is assumed to be the initial planned speed. Due to instrumentation problems, normal accelerations were obtained only during tests involving forward speed.

### Drop Tests Without Forward Speed

Nineteen runs were conducted with no forward speed. Typical time histories of pertinent parameters are presented in figure 5. The time of initial model release is identified as well as the time of model

impact. The stability of the model is demonstrated through the behavior of the measured parameters just after impact. In all tests, the model settled down from the impact in a short period of time, usually only 2 to 3 cycles. This behavior is also seen throughout the data presented in reference 6.

Figure 6 shows the maximum response of the model to the impacts as a function of drop height and initial pitch angle. Figure 6(a) shows that the maximum front-lobe pressure increased with increasing drop height. This is indicative of increased potential energy in the system. In this report only the front-lobe and the right-side-lobe pressures were measured and presented, since they are the lobes that would be expected to experience the highest pressures. Front-lobe pressure also increased with increasing initial pitch angle. This was due in part to increased center-of-gravity height at a fixed drop height as initial pitch angle increased. The maximum front-lobe pressure experienced was 1.6 psig.

In figure 6(b), the maximum side-lobe pressure also increased with increasing drop height, very much like the front-lobe pressure. However, the side-lobe pressure appears to be insensitive to initial pitch angle. The maximum side-lobe pressure experienced was 1.1 psig.

The sensitivity of the maximum cavity pressure shown in figure 6(c) seems to be inversely related to initial pitch angle. This trend is attributed to the cavity being open to the atmosphere for a longer period of time as the initial pitch angle is increased, thereby allowing the lobes to absorb more of the impact energy before sealing the cavity.

Figure 6(d) shows that the maximum normal acceleration of the model (with a forward speed of 5 ft/sec) increased both with drop height and initial pitch angle. Again, this behavior is expected because of increased center-of-gravity height for either increased drop height or initial pitch angle. This plot is presented at a nominal speed of 5 ft/sec, since no normal acceleration data were obtained for tests without forward speed.

The center of pressure of the air bag was forward of the center of gravity of the model, just as in the full-scale vehicle. Consequently, at 0° initial pitch angle, increasing drop height produced increased maximum pitch-up behavior of the model. (See fig. 6(e).) However, at initial pitch-up attitudes of 5°, 10°, and 15°, the maximum pitch deflection of the model was in the nose-down direction. Drop height apparently did not significantly affect the maximum nose-down attitude of the model except for the 0° initial-pitch-angle tests. A maximum pitch deflection of approximately −4.5° occurred at a 6-in. drop height with 15° initial pitch angle. The effect of drop height and initial pitch angle on maximum roll angle is presented in figure 6(f); however, there are no significant trends or maximum deflections.

Figure 6(g) shows the maximum vertical displacement of the center of gravity of the model as a function of drop height and initial pitch angle. The maximum vertical displacement increased as drop height increased regardless of initial pitch angle. However, the data obtained for an initial pitch angle of 15° show a reduction of the maximum vertical displacement compared with the data obtained for an initial pitch angle of 10°.

Shown in figure 7 are the effects of initial roll angle and drop height on various model parameters. Figure 7(a) illustrates the effect of initial roll angle and drop height on the maximum cavity pressure. For all cases, increasing initial roll angle decreased the maximum cavity pressure. This behavior is similar to that of the pitch data, indicating increased air-bag lobe absorbtion of the impact energy. As expected, increasing the drop height increased the maximum cavity pressure, with a maximum of just under 1 psig occurring in a 6-in. drop-height test with 0° initial roll angle.

Figure 7(b) shows the effect of initial roll angle and drop height on the maximum normal acceleration. The data show the model to be well-behaved and following the expected response. The maximum normal acceleration increased with drop height and appeared to be insensitive to initial roll angle. Again, this plot is presented at a nominal speed of 5 ft/sec, since no acceleration data were obtained for tests without forward speed.

Figure 7(c) gives the maximum roll angle as a function of initial roll angle and drop height. Drop height had no effect on the maximum roll angle at impact, whereas increasing initial roll angle produced increasing roll response after impact in the opposite direction. The maximum roll angle obtained was approximately −1.8°, which occurred for an initial roll angle of 5°.

Initial roll angle had no effect on either maximum front-lobe pressure or maximum side-lobe pressure. The effect of drop height on these parameters was discussed previously.

## Drop Tests With Forward Speed

Data showing the effect of forward speed are presented in figure 8. All the plots in figure 8 are obtained at a nominal drop height of 4 in.

Figures 8(a) and 8(b) present the effect of forward speed and initial pitch angle on the maximum front- and side-lobe pressures, respectively. The maximum front-lobe pressure was not affected by forward

speed. The maximum side-lobe pressure increased with increasing forward speed; however, the mechanism for this is not known.

The effect of forward speed and initial pitch angle on maximum cavity pressure is shown in figure 8(c). Forward speed had no effect on this parameter, and in fact may have masked the behavior of the maximum cavity pressure as a function of initial pitch angle as previously shown in figure 6(c).

Figure 8(d) shows the effect of forward speed and initial pitch angle on maximum normal acceleration. The data show that increasing initial pitch angle increased the maximum normal acceleration from an average of $6g$ for the 0° initial-pitch-angle tests to an average of $8g$ for the 15° initial-pitch-angle tests ($1g = 32.2$ ft/sec$^2$). Forward speed had no effect on the maximum normal acceleration of the system. Based on the fact that the pressures and vertical displacements of the model are essentially unaffected by forward speed, it may be assumed that the normal accelerations in tests without forward speed are the same as those in tests with forward speed.

Figure 8(e) shows that forward speed had no effect on the maximum vertical displacement of the model. The trend of the effect of initial pitch angle on the maximum vertical displacement is similar to that seen in figure 6(g).

Figure 8(f) shows the effect of forward speed and initial pitch angle on the maximum pitch angle after impact. The trends of this parameter as a function of initial pitch angle are essentially the same as those shown in figure 6(e). However, increasing forward speed appears to increase the maximum nose-down pitch angle of the model at impact. Except for the 0° initial-pitch-angle tests, the maximum nose-down pitch angle of the model doubles over the speed range tested.

## Concluding Remarks

An experimental investigation was conducted at the NASA Langley Research Center to determine the effects of various parameters on the impact performance of a 1/3-scale dynamic model of an air cushion vehicle. The parameters studied include drop height, initial pitch angle, initial roll angle, and forward speed. Impact performance was evaluated by measuring the maximum values of variables, including side-lobe, front-lobe, and cavity pressures, normal acceleration, pitch and roll angles after impact, and vertical displacement at impact.

In general, increasing initial pitch angle increased the maximum values of several variables. These include front-lobe pressure, normal acceleration, nose-down pitch angle, and to some extent, vertical displacement. Maximum cavity pressure was inversely affected by increasing initial pitch angle.

Initial roll angle caused a change in sign and increase of the maximum roll angle after impact, but it had no effect on the maximum normal acceleration.

Increasing the drop height of the model increased the potential energy of the system and produced, in general, larger responses over the entire range of variables measured. Increasing drop height increased the maximum value of all pressures, normal acceleration, nose-down pitch at impact, and vertical displacement, while the roll angle at impact remained essentially constant.

Generally, forward speed had no effect on the maximum values of the measured variables. Normal acceleration data were not obtained for tests without forward speed. However, based on the fact that pressures and vertical displacements remained nearly constant over the entire speed range, it may be assumed that the normal accelerations without forward speed are the same as those with forward speed. For tests involving an initial pitch angle, the maximum forward speed of 15 ft/sec generally had the effect of doubling the maximum nose-down pitch angle at impact.

NASA Langley Research Center
Hampton, VA 23665
January 28, 1985

## References

1. Helm, R. W.: Initial Experience With a Three Plenum Cell Air Cushion Equipment Transporter. *Seventeenth Canadian Symposium on Air Cushion Technology—Preprints*, Air Cushion Technol. Soc., Canadian Aeronaut. & Space Inst., c.1983, p. 71.
2. Saha, Hrishikesh, compiler: *Air Cushion Landing Systems*. Univ. of Tennessee Space Inst., c.1973.
3. Markham, P. de L.; Laframboise, J. E.; and Ball, M. A.: Canadian Coast Guard ACIB—1982/83 Trials. *Seventeenth Canadian Symposium on Air Cushion Technology—Preprints*, Air Cushion Technol. Soc., Canadian Aeronaut. & Space Inst., c.1983, pp. 60–68.
4. Daugherty, Robert H.: *Braking and Cornering Studies on an Air Cushion Landing System*. NASA TP-2196, 1983.
5. Tanner, John A.: *Fore-and-Aft Elastic Response Characteristics of* $34 \times 9.9$, *Type VII, 14 Ply-Rating Aircraft Tires of Bias-Ply, Bias-Belted, and Radial-Belted Design*. NASA TN D-7449, 1974.
6. Leland, Trafford J. W.; Thompson, William C.; and Vohringer, David S.: IV/3. Preliminary Results From Dynamic Model Tests of an Air Cushion Landing System. *Air Cushion Landing Systems*, Hrishikesh Saha, compiler, Univ. of Tennessee Space Inst., c.1973, pp. 479–510.

TABLE I. SCALING

| Quantity | Full-scale value | Scale factor | Model value |
|---|---|---|---|
| Length | $L$ | $\lambda$ | $\lambda L$ |
| Force | $F$ | $\lambda^3$ | $\lambda^3 F$ |
| Moment of inertia | $I$ | $\lambda^5$ | $\lambda^5 I$ |
| Mass | $M$ | $\lambda^3$ | $\lambda^3 M$ |
| Time | $T$ | $\sqrt{\lambda}$ | $\sqrt{\lambda} T$ |
| Speed | $V$ | $\sqrt{\lambda}$ | $\sqrt{\lambda} V$ |
| Linear accelerations | $A$ | 1 | $A$ |
| Pressure | $P$ | $\lambda$ | $\lambda P$ |

TABLE II. FULL-SCALE VEHICLE AND MODEL INFORMATION

| Parameter | Full-scale value | 1/3-scale model actual value |
|---|---|---|
| Air-bag length, in. | 169 | 59 |
| Air-bag width, in. | 97 | 33 |
| Weight, lb | 5500 | 204 |
| Pitch inertia, slug/ft$^2$ | 3921 | 16.5 |
| Roll inertia, slug/ft$^2$ | 1205 | 4.9 |
| Center-of-gravity height, in. | 41 | 13 |
| Nominal lobe pressure, lb/in$^2$ | 0.8 | 0.4 |
| Nominal cavity pressure, lb/in$^2$ | 0.4 | 0.1 |
| Nominal airflow, lbm/sec | 6.0 | 0.4 |

TABLE III. SUMMARY OF 1/3-SCALE-MODEL TEST CONDITIONS AND RESULTS

| Run number | Initial conditions | | | | Maximum values | | | | | | | |
|---|---|---|---|---|---|---|---|---|---|---|---|---|
| | Forward speed, ft/sec | Pitch angle, deg | Roll angle, deg | Drop height, in. | Side-lobe pressure, psig | Front-lobe pressure, psig | Cavity pressure, psig | Normal acceleration, $g$ units | Roll angle, deg | Pitch angle, deg | Vertical displacement, in. | Forward speed, ft/sec |
| 1 | 0 | 0 | 0 | 2 | 0.7 | 0.7 | 0.5 | | 1.0 | −1.1 | 0.7 | 0 |
| 2 | 0 | 0 | 0 | 4 | .9 | .9 | .8 | | 1.1 | .8 | .8 | 0 |
| 3 | 0 | 0 | 0 | 6 | 1.1 | 1.1 | 1.0 | | .7 | 1.1 | .9 | 0 |
| 4 | 0 | 0 | 0 | 8 | 1.3 | 1.2 | 1.1 | | .6 | 1.2 | 1.2 | 0 |
| 5 | 0 | 5 | 0 | 2 | .8 | .9 | .5 | | −.5 | −1.9 | 1.0 | 0 |
| 6 | 0 | 5 | 0 | 4 | .9 | 1.0 | .7 | | −.4 | −1.7 | 1.1 | 0 |
| 7 | 0 | 5 | 0 | 6 | 1.1 | 1.2 | .8 | | −.4 | −1.7 | 1.3 | 0 |
| 8 | 0 | 10 | 0 | 2 | .8 | 1.2 | .6 | | −.7 | −3.4 | 1.1 | 0 |
| 9 | 0 | 10 | 0 | 4 | .9 | 1.2 | .7 | | −.7 | −3.4 | 1.3 | 0 |
| 10 | 0 | 10 | 0 | 6 | 1.0 | 1.3 | .7 | | −.9 | −3.2 | 1.6 | 0 |
| 11 | 0 | 15 | 0 | 2 | .9 | 1.3 | .5 | | −1.1 | −4.1 | .8 | 0 |
| 12 | 0 | 15 | 0 | 4 | 1.0 | 1.3 | .6 | | −1.3 | −4.5 | 1.1 | 0 |
| 13 | 0 | 15 | 0 | 6 | 1.0 | 1.6 | .7 | | −1.3 | −4.7 | 1.6 | 0 |
| 14 | 0 | 0 | 5 | 2 | .8 | .8 | .5 | | −1.7 | −1.8 | .9 | 0 |
| 15 | 0 | 0 | 5 | 4 | .9 | .9 | .6 | | −1.7 | 2.0 | 1.0 | 0 |
| 16 | 0 | 0 | 5 | 6 | 1.1 | 1.1 | .7 | | −1.7 | 1.6 | 1.1 | 0 |
| 17 | 0 | 5 | 5 | 4 | .9 | 1.0 | .7 | | −1.3 | −1.1 | 1.3 | 0 |
| 18 | 0 | 10 | 5 | 4 | .9 | 1.2 | .7 | | −1.4 | −9.4 | 1.8 | 0 |
| 19 | 0 | 15 | 5 | 4 | .9 | | .7 | | −1.6 | −4.1 | 1.9 | 0 |
| 20 | 5 | 0 | 0 | 2 | .7 | .8 | .6 | 4.2 | .8 | .6 | .7 | 5.3 |
| 21 | 10 | 0 | 0 | 2 | .7 | .8 | .6 | 4.3 | .7 | 1.1 | .9 | 9.6 |
| 22 | 15 | 0 | 0 | 2 | .7 | .8 | .6 | 4.8 | 1.2 | 1.4 | 1.0 | 14.0 |
| 23 | 5 | 0 | 0 | 4 | 1.0 | 1.0 | .9 | 6.7 | 1.1 | .8 | 1.2 | 5.0 |
| 24 | 10 | 0 | 0 | 4 | .9 | 1.0 | .8 | 5.8 | 1.3 | 1.2 | 1.0 | 10.1 |
| 25 | 15 | 0 | 0 | 4 | .9 | .9 | .7 | 5.7 | 1.1 | 1.0 | .9 | 14.6 |
| 26 | 5 | 0 | 0 | 6 | 1.1 | 1.1 | 1.0 | 7.0 | .9 | 1.6 | 1.1 | 5.4 |
| 27 | 10 | 0 | 0 | 6 | 1.1 | 1.1 | .9 | 7.0 | 1.2 | .9 | 1.1 | 9.6 |
| 28 | 15 | 0 | 0 | 6 | 1.0 | 1.1 | .9 | 6.8 | 1.4 | 1.1 | 1.0 | 14.6 |
| 29 | 5 | 5 | 0 | 2 | 1.0 | 1.2 | .7 | 6.9 | 1.2 | −2.9 | 1.1 | 4.9 |
| 30 | 10 | 5 | 0 | 2 | .9 | 1.3 | .7 | 6.1 | .8 | −3.4 | 1.0 | 8.2 |
| 31 | 15 | 5 | 0 | 2 | .9 | 1.2 | .7 | 5.9 | .3 | −4.1 | .8 | 12.4 |
| 32 | 5 | 5 | 0 | 4 | 1.1 | 1.3 | .9 | 7.1 | .8 | −3.3 | 1.2 | 4.4 |
| 33 | 10 | 5 | 0 | 4 | 1.1 | 1.3 | .9 | 7.3 | .4 | −3.4 | 1.2 | 8.3 |

TABLE III. Concluded

| Run number | Initial conditions | | | | Maximum values | | | | | | | |
|---|---|---|---|---|---|---|---|---|---|---|---|---|
| | Forward speed, ft/sec | Pitch angle, deg | Roll angle, deg | Drop height, in. | Side-lobe pressure, psig | Front-lobe pressure, psig | Cavity pressure, psig | Normal acceleration, $g$ units | Roll angle, deg | Pitch angle, deg | Vertical displacement, in. | Forward speed, ft/sec |
| 34 | 15 | 5 | 0 | 4 | 1.1 | 1.3 | 0.9 | 7.3 | 1.1 | −7.0 | 1.2 | 12.0 |
| 35 | 5 | 5 | 0 | 6 | 1.1 | 1.3 | 1.0 | 8.1 | .2 | −4.4 | 1.3 | 4.4 |
| 36 | 10 | 5 | 0 | 6 | 1.3 | 1.3 | 1.2 | 8.4 | .7 | −5.7 | 1.5 | 8.2 |
| 37 | 15 | 5 | 0 | 6 | 1.2 | 1.4 | 1.0 | 7.9 | .8 | −5.7 | 1.5 | 11.8 |
| 38 | 5 | 10 | 0 | 2 | 1.1 | 1.7 | .8 | 6.7 | .4 | −7.3 | 1.1 | 4.2 |
| 39 | 10 | 10 | 0 | 2 | 1.0 | 1.7 | .7 | 6.8 | .0 | −7.4 | 1.1 | 8.2 |
| 40 | 15 | 10 | 0 | 2 | 1.1 | 1.6 | .8 | 6.7 | .5 | −7.9 | 1.2 | 16.1 |
| 41 | 5 | 10 | 0 | 4 | 1.1 | 1.4 | .9 | 7.6 | .8 | −8.3 | 1.3 | 4.3 |
| 42 | 10 | 10 | 0 | 4 | 1.2 | 1.3 | .9 | 7.9 | .5 | −10.3 | 1.3 | |
| 43 | 15 | 10 | 0 | 4 | 1.2 | 1.3 | .9 | 7.8 | .5 | −9.8 | 1.2 | |
| 44 | 5 | 10 | 0 | 6 | 1.2 | 1.4 | 1.0 | 8.0 | 1.0 | −11.1 | 1.4 | |
| 45 | 10 | 10 | 0 | 6 | 1.2 | 1.5 | .9 | 8.3 | .8 | −11.8 | 1.7 | |
| 46 | 15 | 10 | 0 | 6 | 1.3 | 1.4 | .9 | 8.3 | .8 | −10.4 | 1.7 | |
| 47 | 5 | 15 | 0 | 2 | 1.1 | 1.3 | .9 | 7.0 | .9 | −7.5 | 1.4 | |
| 48 | 10 | 15 | 0 | 2 | 1.2 | 1.3 | .8 | 8.3 | .5 | −7.3 | 1.0 | |
| 49 | 15 | 15 | 0 | 2 | 1.1 | 1.3 | .8 | 6.0 | | −7.6 | 1.1 | |
| 50 | 5 | 15 | 0 | 4 | 1.3 | 1.4 | 1.0 | 8.0 | .8 | −9.8 | 1.5 | |
| 51 | 10 | 15 | 0 | 4 | 1.3 | 1.4 | .9 | 8.0 | | −9.8 | 1.5 | |
| 52 | 15 | 15 | 0 | 4 | 1.3 | 1.4 | 1.0 | 8.0 | 1.8 | −9.6 | 1.6 | |
| 53 | 5 | 15 | 0 | 6 | 1.2 | 1.5 | 1.0 | 9.3 | .4 | −10.0 | 1.5 | |
| 54 | 10 | 15 | 0 | 6 | 1.3 | 1.4 | 1.0 | 10.0 | .6 | −11.1 | 1.4 | |
| 55 | 15 | 15 | 0 | 6 | 1.4 | 1.4 | 1.1 | 9.4 | .8 | −14.0 | 2.0 | |
| 56 | 5 | 0 | 5 | 2 | .8 | .8 | .5 | 4.4 | −1.8 | .6 | 1.2 | |
| 57 | 10 | 0 | 5 | 2 | .8 | .8 | .6 | 4.0 | −1.7 | 1.3 | 1.4 | |
| 58 | 15 | 0 | 5 | 2 | .8 | .8 | .5 | 3.8 | −.8 | 1.0 | 1.0 | |
| 59 | 5 | 0 | 5 | 4 | 1.0 | 1.0 | .7 | 6.4 | −.8 | .8 | 1.4 | |
| 60 | 10 | 0 | 5 | 4 | 1.0 | 1.0 | .8 | 7.0 | −.8 | 1.1 | .9 | |
| 61 | 15 | 0 | 5 | 4 | 1.0 | 1.0 | .8 | 6.5 | −2.2 | 1.1 | .8 | |
| 62 | 10 | 5 | 5 | 4 | 1.2 | 1.4 | 1.0 | 7.9 | −2.0 | −3.8 | 1.5 | |
| 63 | 10 | 10 | 5 | 4 | 1.2 | 1.4 | .9 | 8.0 | −1.3 | −8.9 | 1.5 | |
| 64 | 10 | 15 | 5 | 4 | 1.4 | 1.4 | 1.0 | 8.0 | −1.5 | −9.8 | 1.8 | |

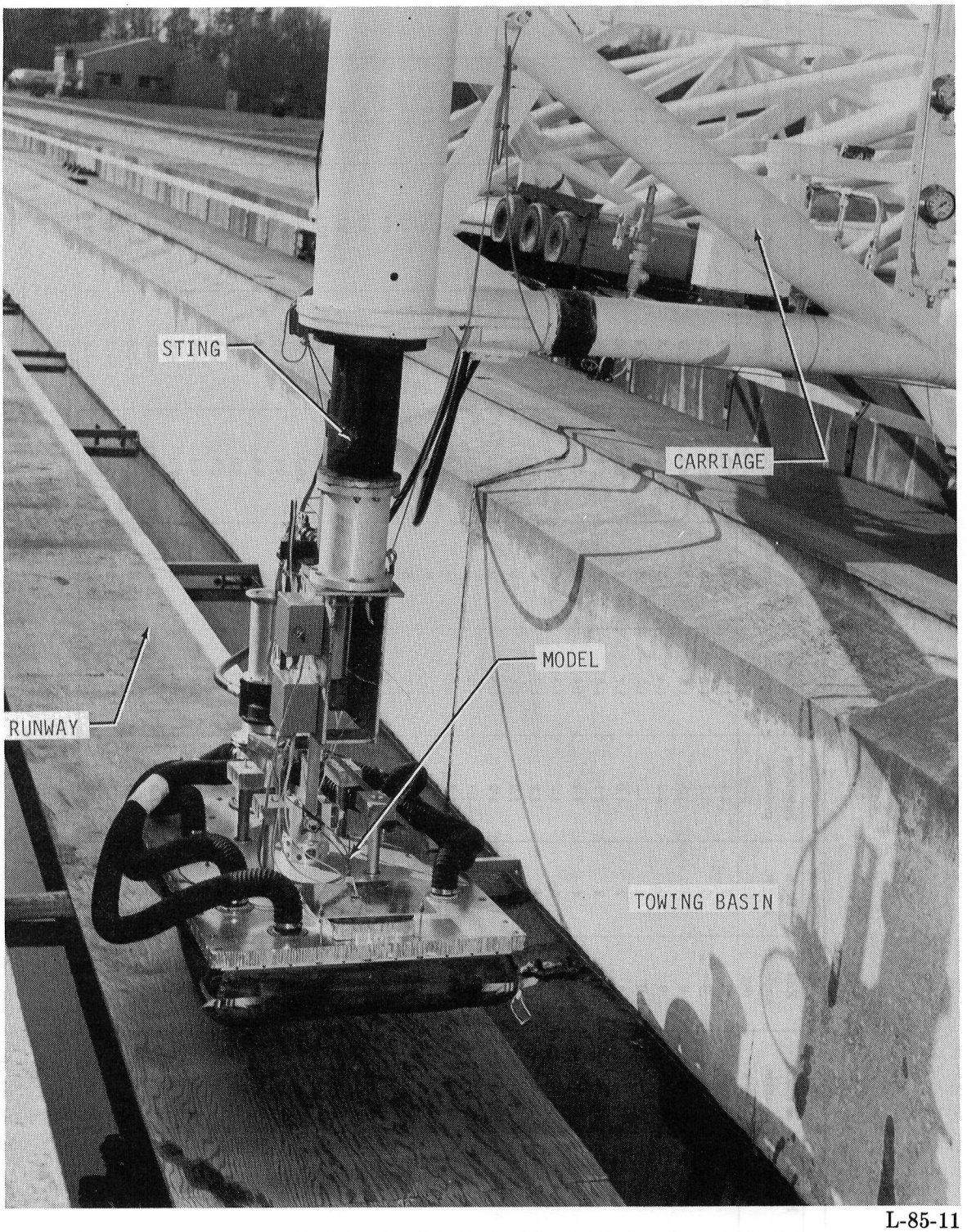


L-85-11

Figure 1. Air cushion model supported on carriage sting.

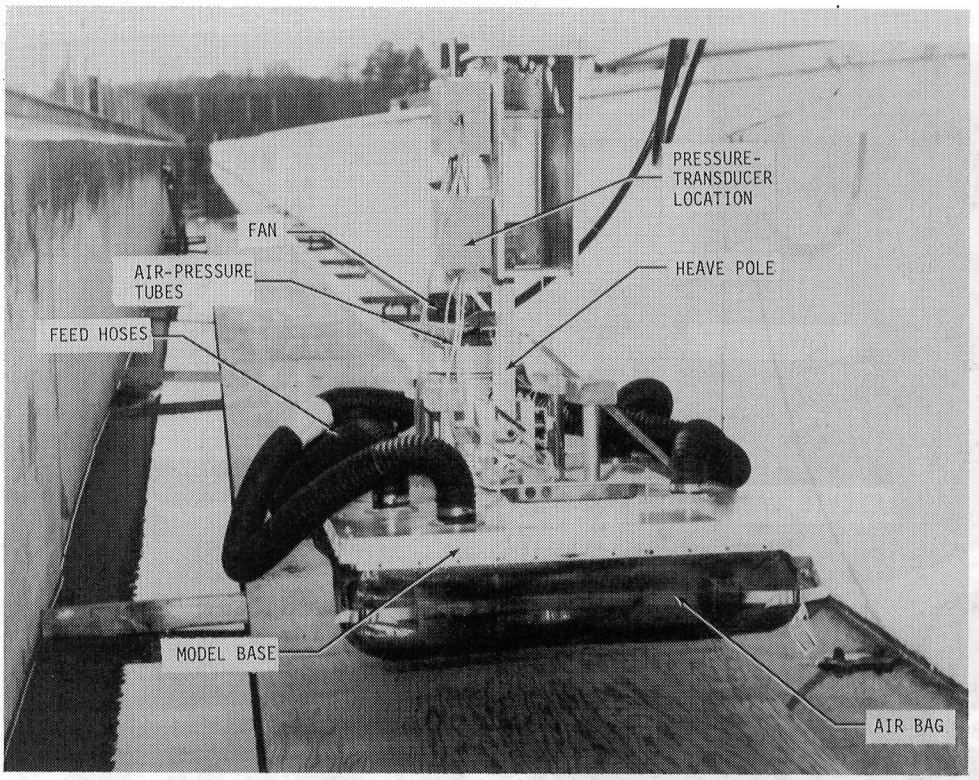


L-85-12

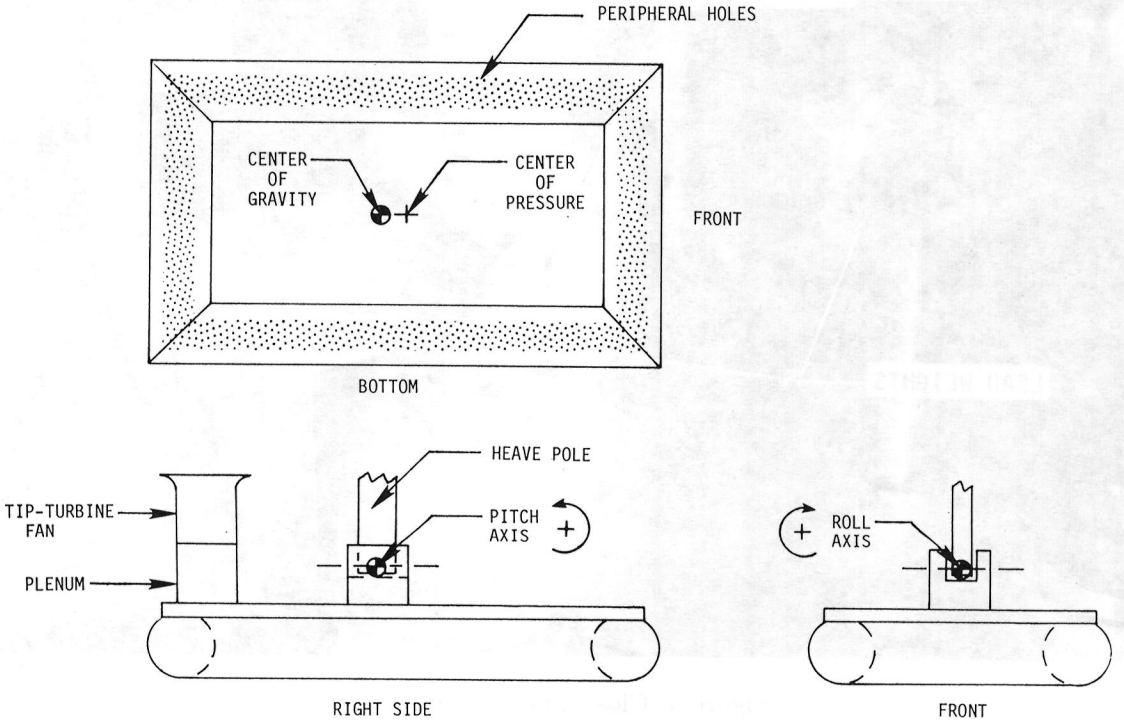


Figure 2. Air cushion model.

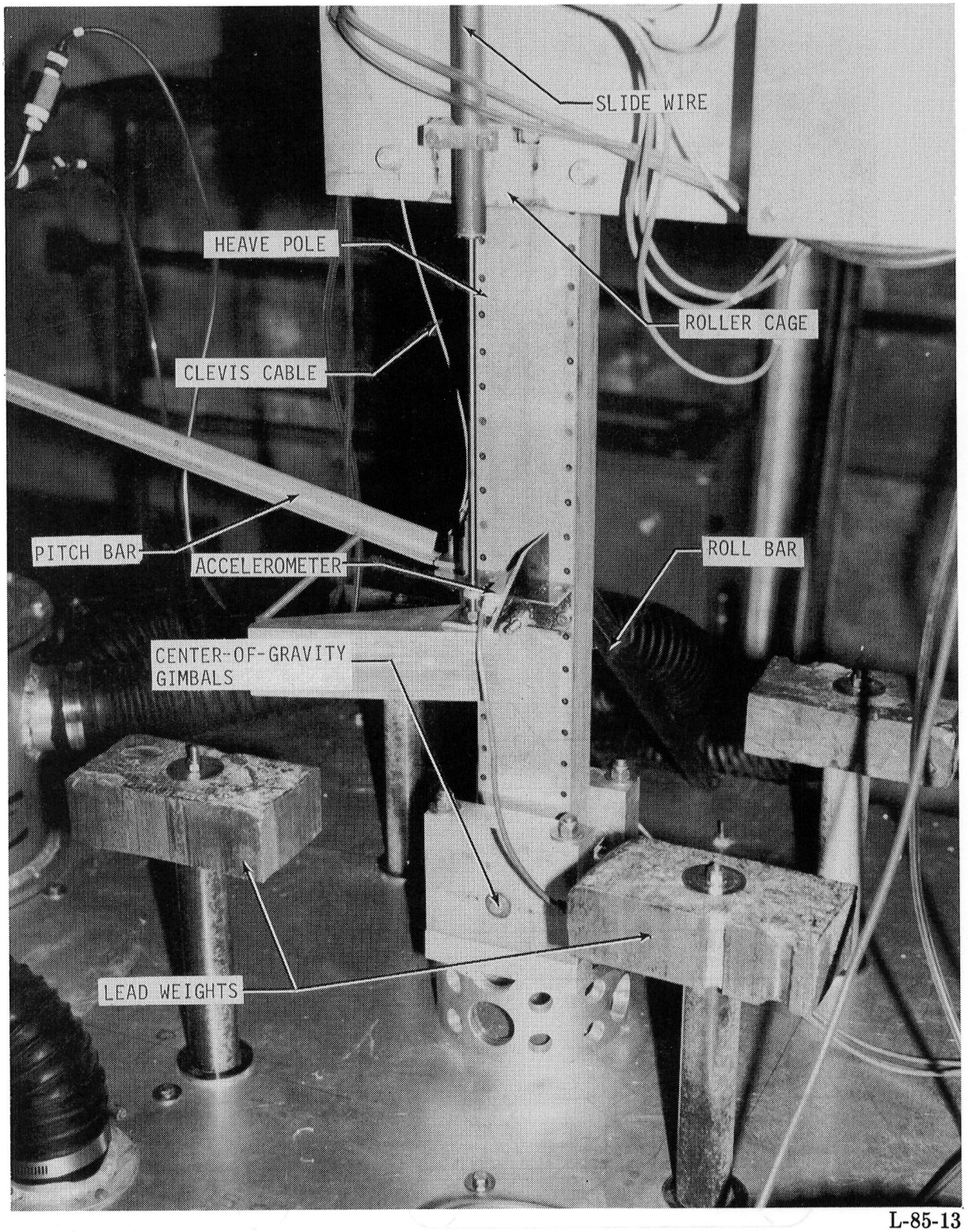


L-85-13

Figure 3. Close-up of model center.

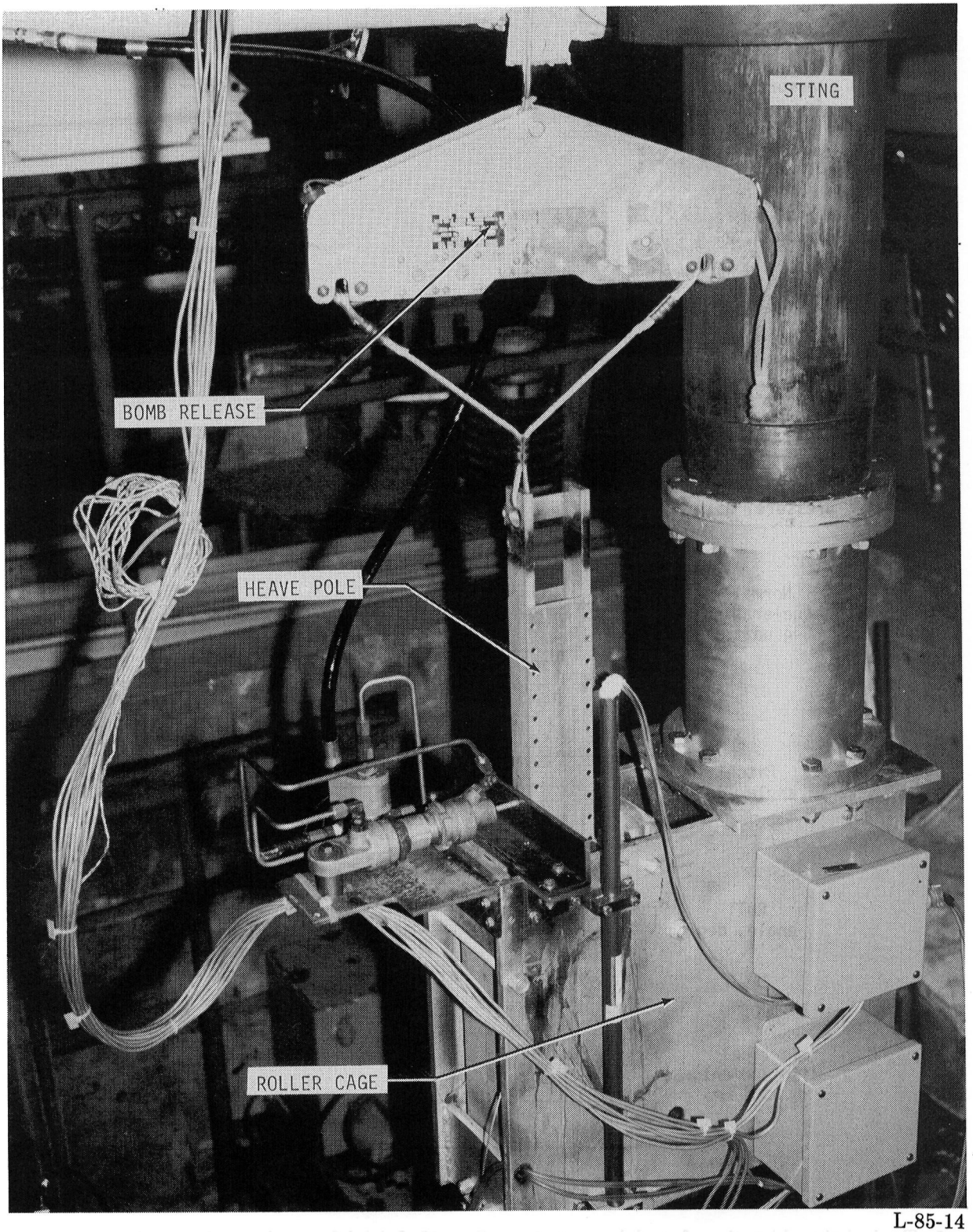


L-85-14

Figure 4. Assembly of bomb release and heave pole.

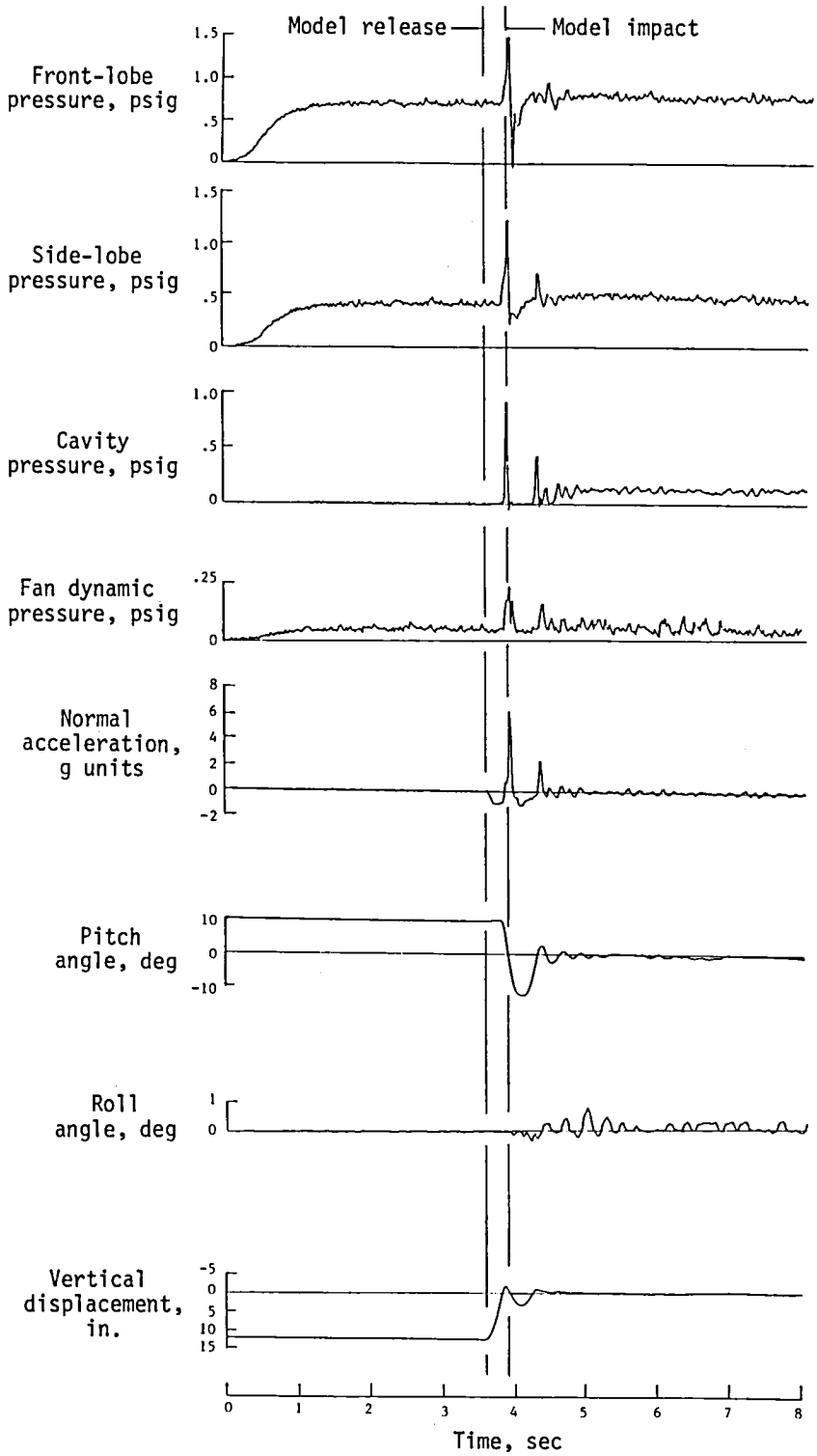


Figure 5. Typical time histories of model parameters. Run 45; Initial forward speed = 10 ft/sec; Initial pitch angle = 10°; Initial roll angle = 0°; Initial drop height = 6 in.

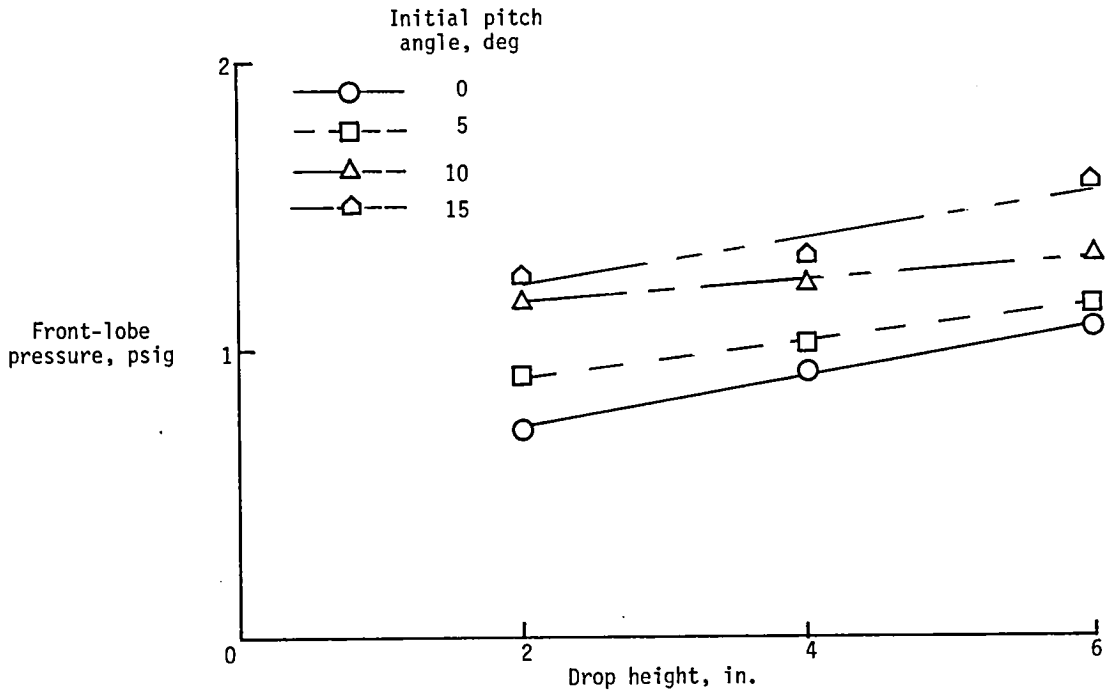


(a) Front-lobe pressure.

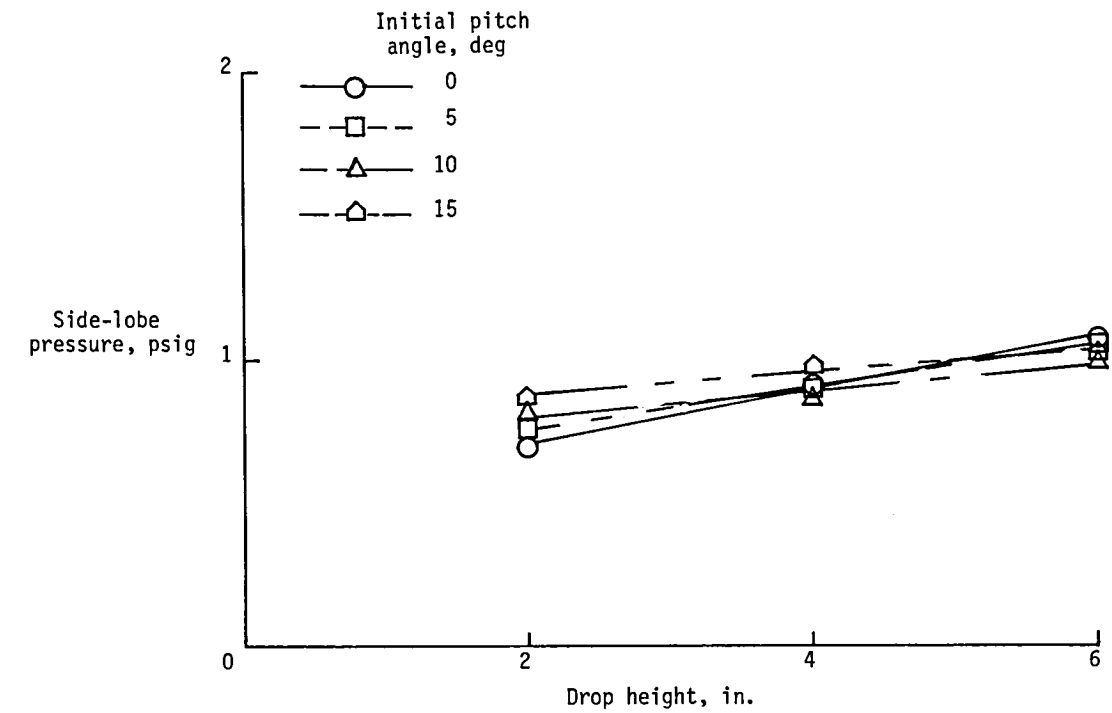


(b) Side-lobe pressure.

Figure 6. Maximum values of model parameters during impact as a function of drop height and initial pitch angle.

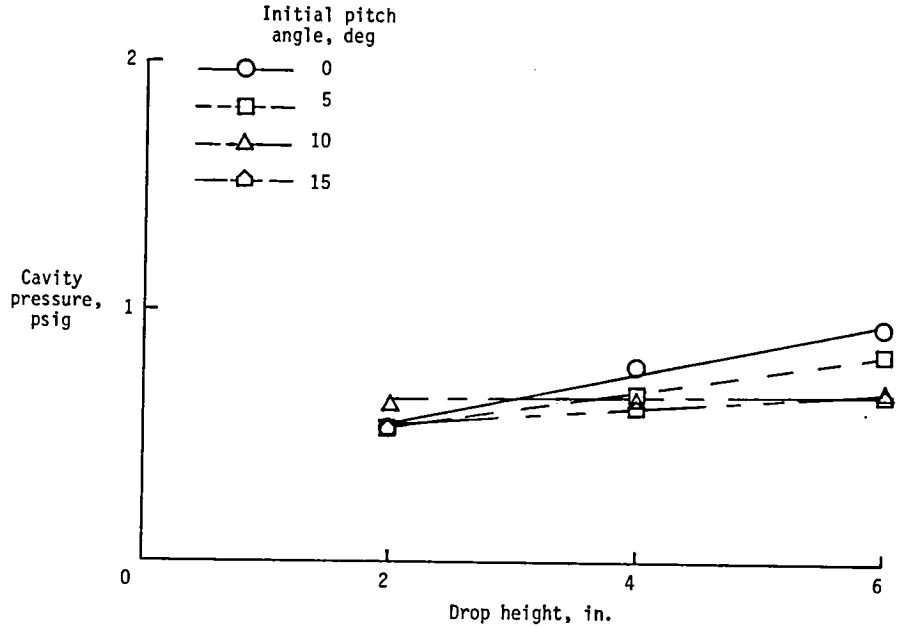


(c) Cavity pressure.

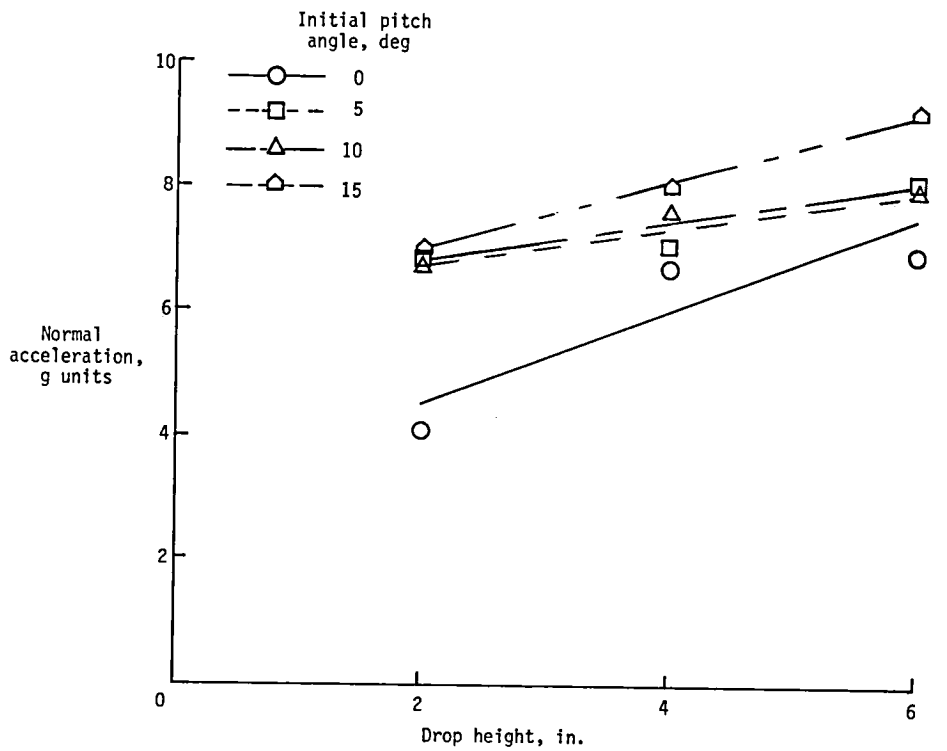


(d) Normal acceleration (5 ft/sec nominal forward speed).

Figure 6. Continued.

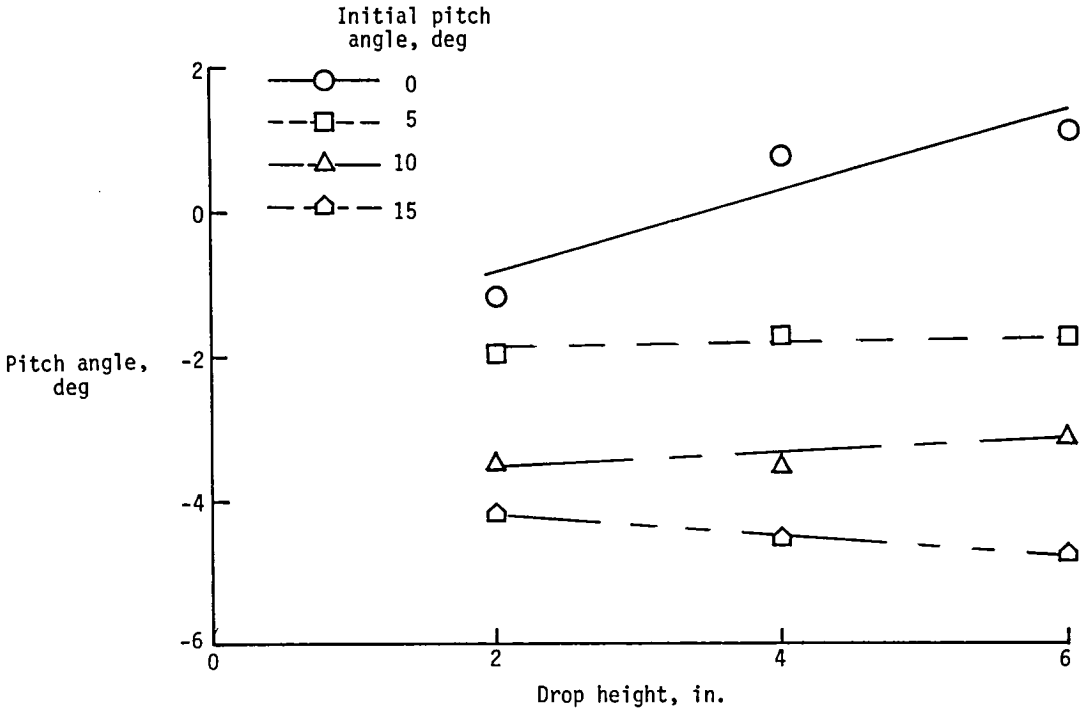


(e) Pitch angle.

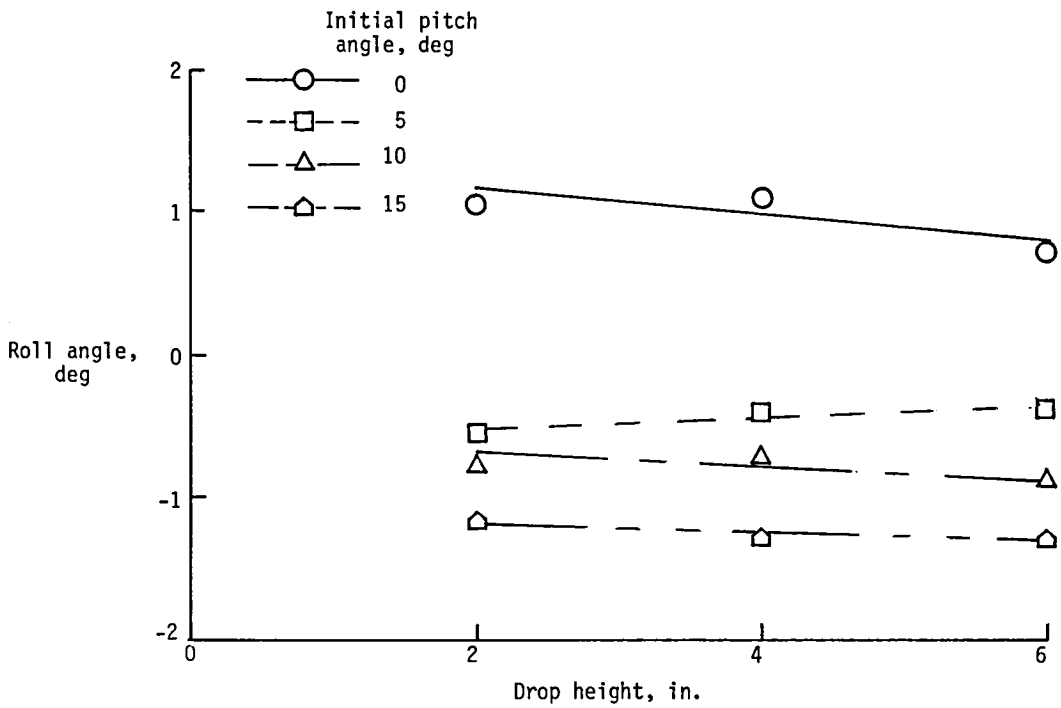


(f) Roll angle.

Figure 6. Continued.

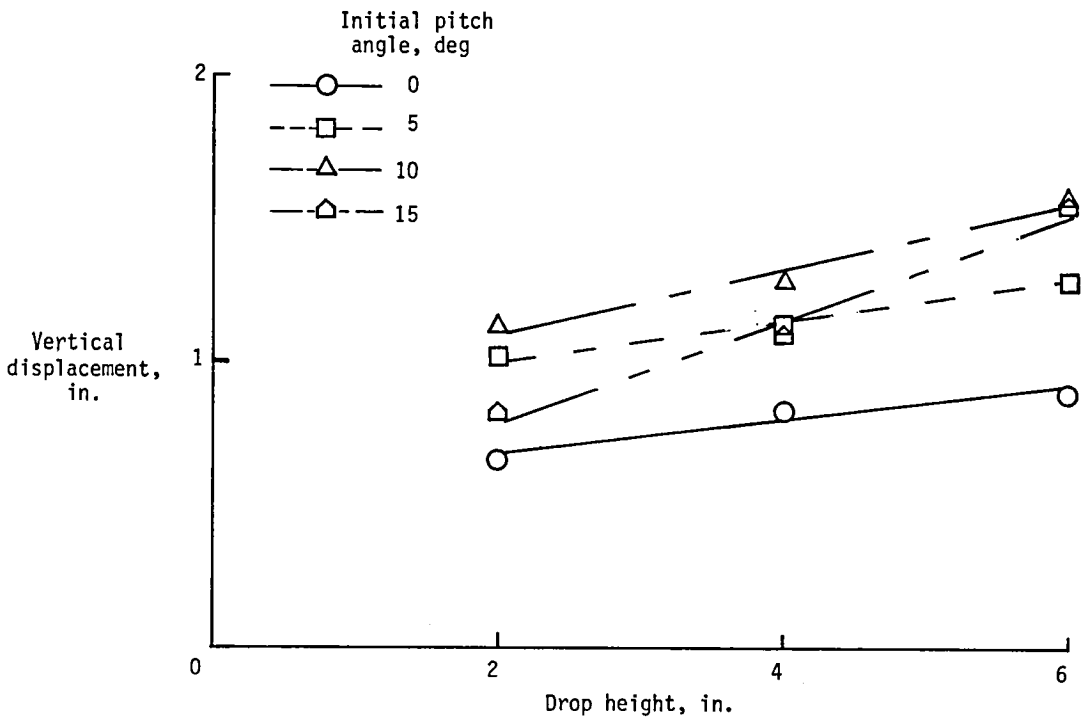


(g) Vertical displacement.

Figure 6. Concluded.

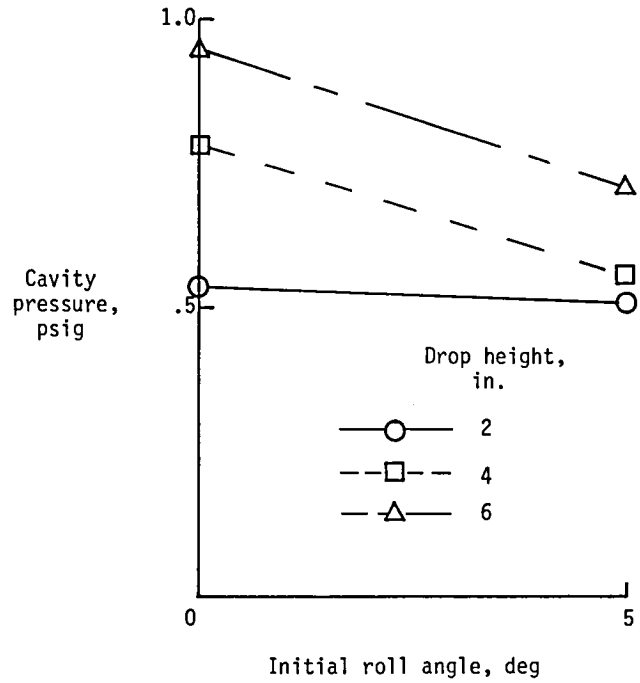


(a) Cavity pressure.

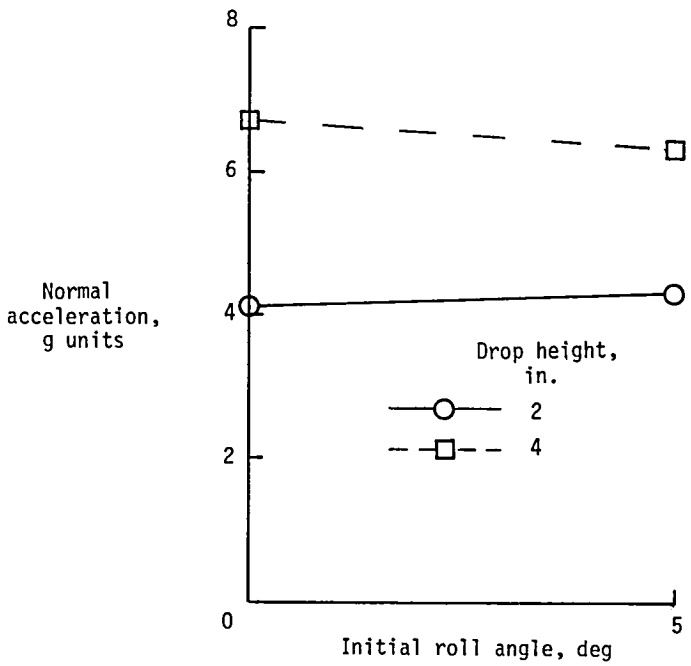


(b) Normal acceleration (5 ft/sec nominal forward speed).

Figure 7. Maximum values of model parameters during impact as a function of initial roll angle and drop height.

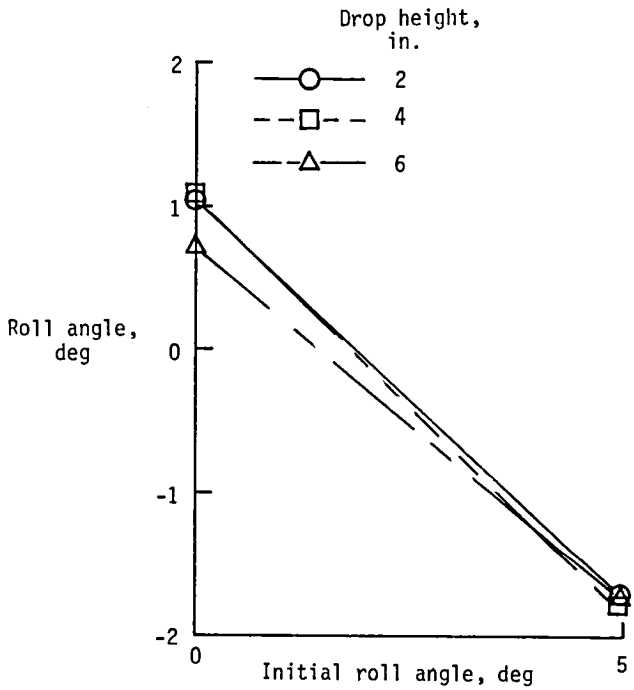


(c) Roll angle.

Figure 7. Concluded.

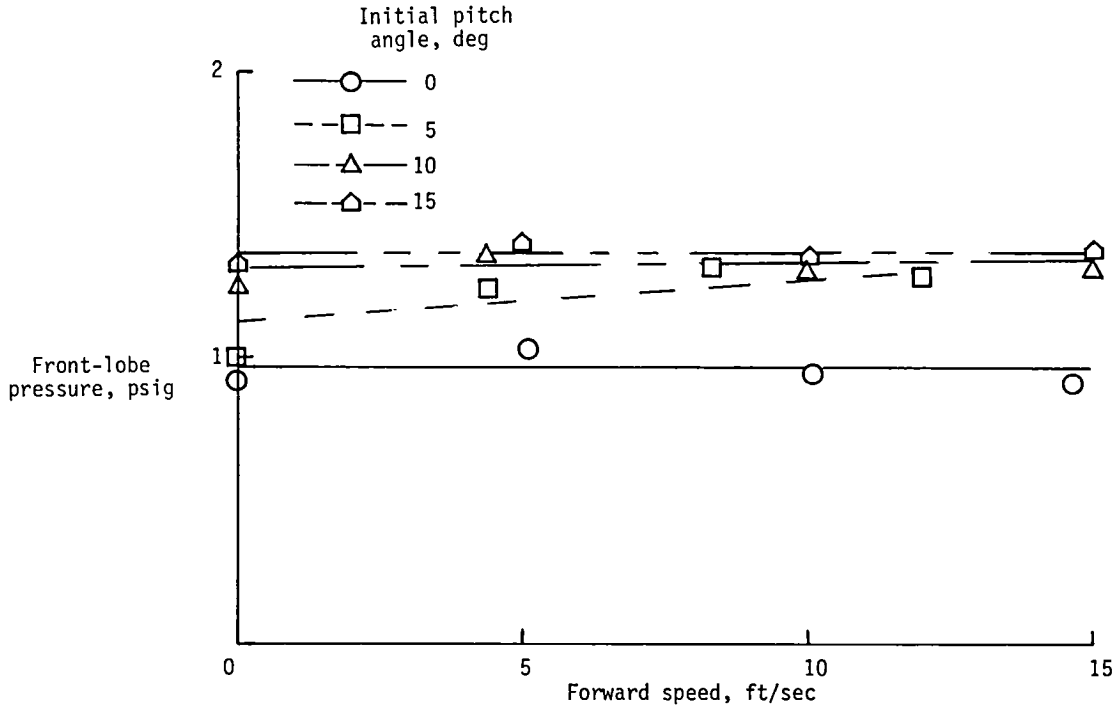


(a) Front-lobe pressure.

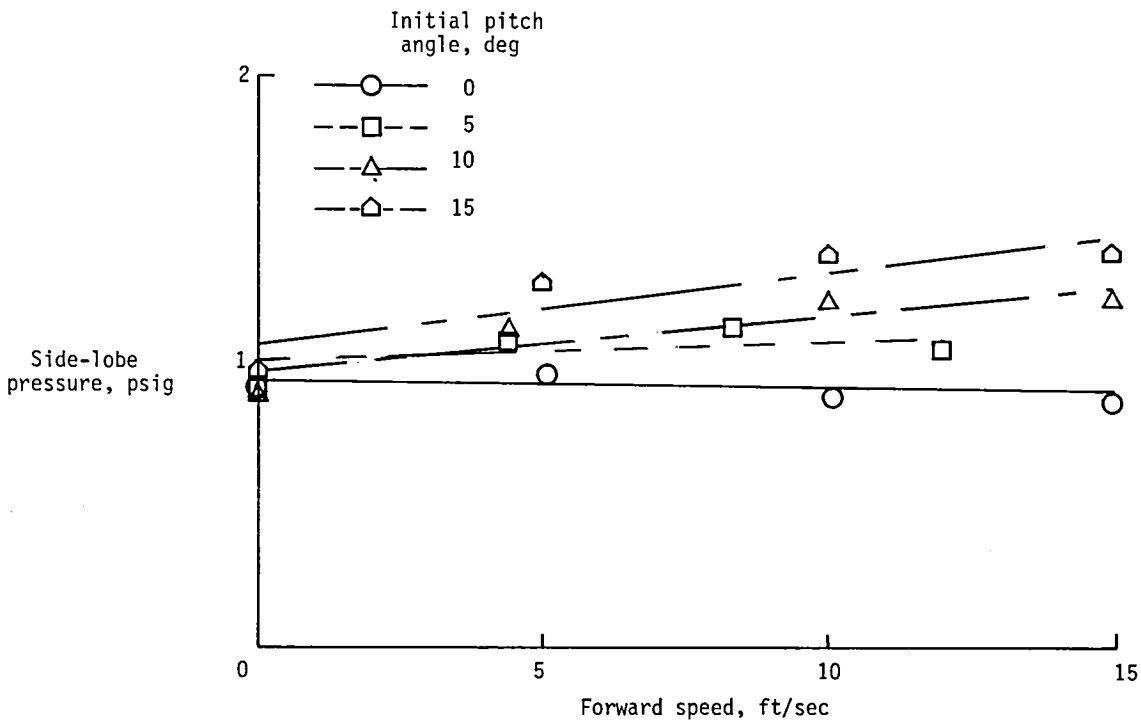


(b) Side-lobe pressure.

Figure 8. Maximum values of model parameters during impact as a function of forward speed and initial pitch angle.

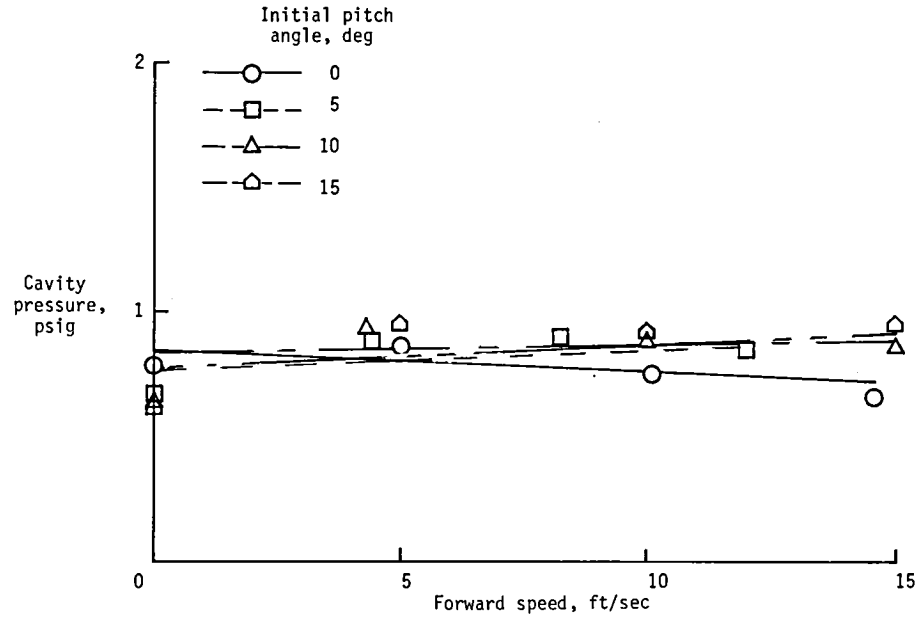


(c) Cavity pressure.

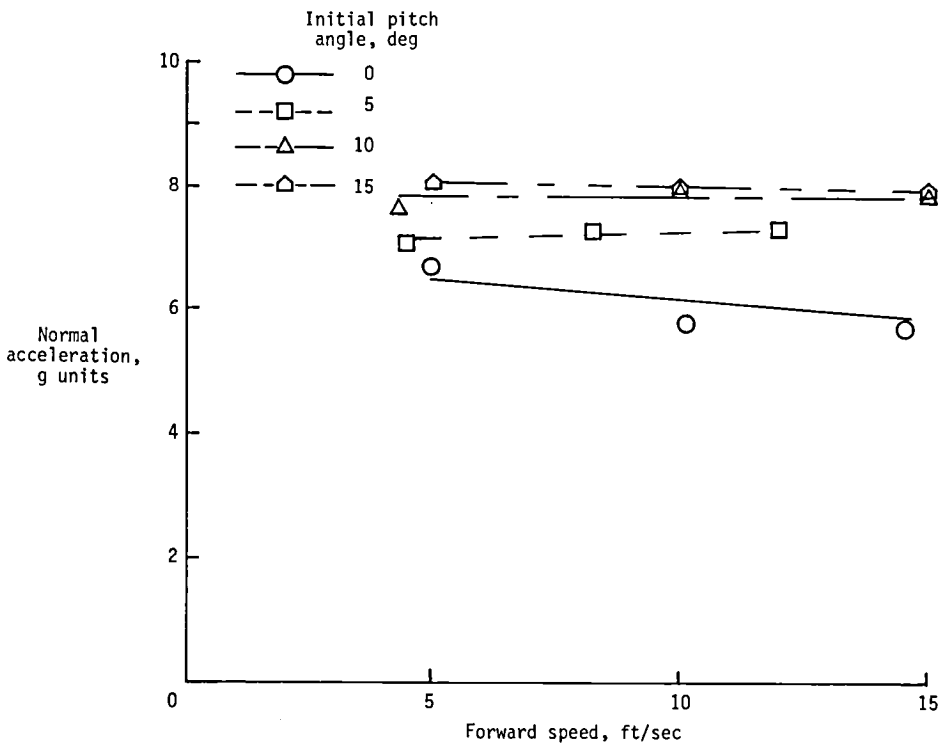


(d) Normal acceleration.

Figure 8. Continued.

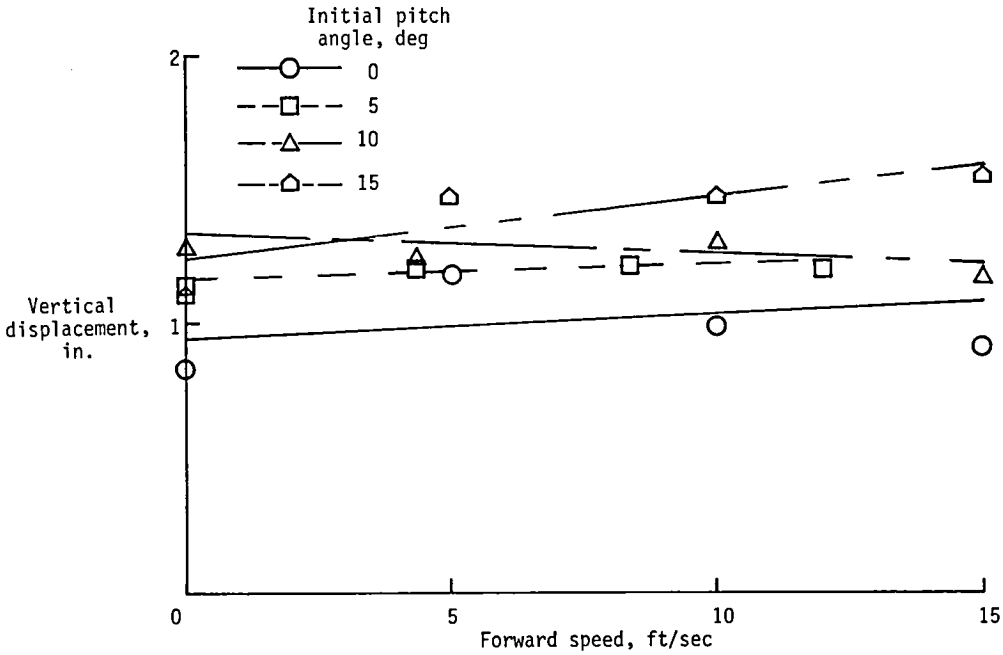


(e) Vertical displacement.

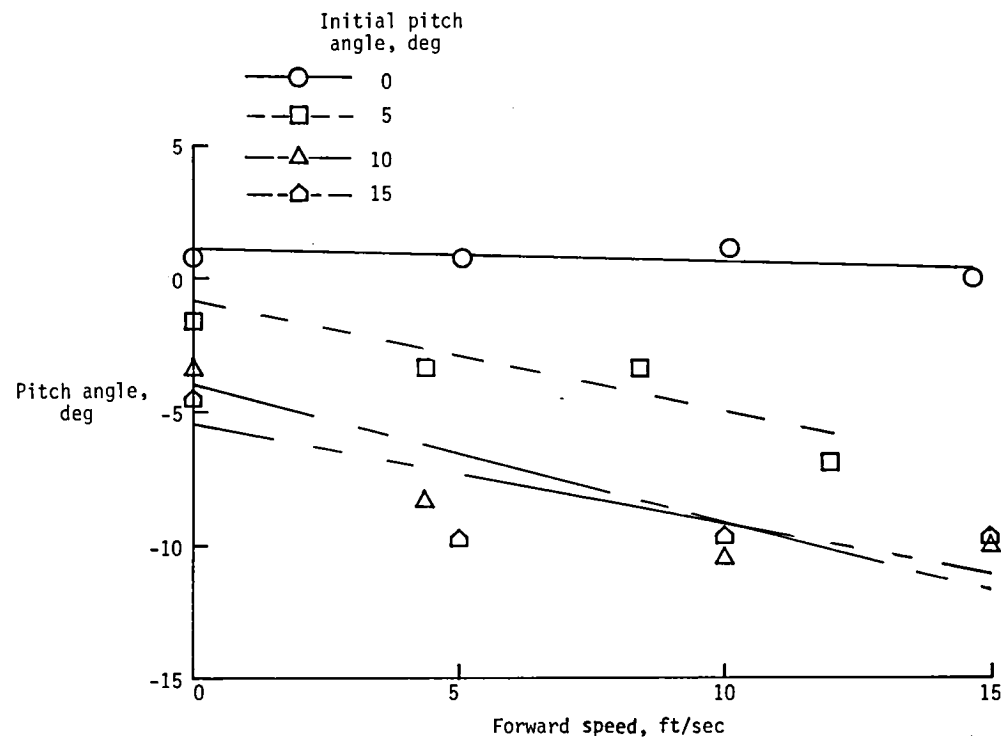


(f) Pitch angle.

Figure 8. Concluded.

| 1. Report No. | 2. Government Accession No. | 3. Recipient's Catalog No. |
|---|---|---|
| NASA TM-86360 | | |

| 4. Title and Subtitle | 5. Report Date |
|---|---|
| Impact Studies of a 1/3-Scale Model of an Air Cushion Vehicle | April 1985 |
| | 6. Performing Organization Code: 505-45-14-01 |
| 7. Author(s): Robert H. Daugherty | 8. Performing Organization Report No.: L-15916 |
| 9. Performing Organization Name and Address: NASA Langley Research Center, Hampton, VA 23665 | 10. Work Unit No. |
| | 11. Contract or Grant No. |
| 12. Sponsoring Agency Name and Address: National Aeronautics and Space Administration, Washington, DC 20546 | 13. Type of Report and Period Covered: Technical Memorandum |
| | 14. Sponsoring Agency Code |

15. Supplementary Notes

16. Abstract

An experimental investigation was conducted at the NASA Langley Research Center to determine the effects of various parameters of the impact performance of a 1/3-scale dynamic model of an air cushion vehicle. Impact response was determined by measuring the maximum values of variables, including side-lobe, front-lobe, and cavity pressures, normal acceleration, pitch and roll angles, and vertical displacement during impact, for various combinations of drop height, initial pitch and roll angles, and forward speed. Increasing initial pitch angle increased the maximum values of the front-lobe pressure, normal acceleration, nose-down pitch angle, and to some extent, vertical displacement, but it inversely affected the maximum cavity pressure. Increasing the drop height of the model increased the potential energy of the system and generally produced larger responses over the entire range of variables measured, except for the roll angle after impact, which remained constant. Forward speed had no effect on the impact performance of the model, except for essentially doubling the maximum nose-down pitch angle after impact at the maximum speed tested.

17. Key Words (Suggested by Authors(s))
Air cushion vehicle
Air bag
Model
Impact
Pressure
Acceleration

18. Distribution Statement
Unclassified—Unlimited

Subject Category 05

| 19. Security Classif.(of this report) | 20. Security Classif.(of this page) | 21. No. of Pages | 22. Price |
|---|---|---|---|
| Unclassified | Unclassified | 23 | A02 |

For sale by the National Technical Information Service, Springfield, Virginia 22161

NASA-Langley, 1985

National Aeronautics and
Space Administration

Washington, D.C.
20546

Official Business
Penalty for Private Use, $300

THIRD-CLASS BULK RATE

Postage and Fees Paid
National Aeronautics and
Space Administration
NASA-451


POSTMASTER: If Undeliverable (Section 158 Postal Manual) Do Not Return